Origins and Diversity of the Aging Reaction in Phosphonate Adducts of Serine Hydrolase Enzymes: What Characteristics of the Active Site Do They Probe?†

Akos Bencsura,‡ Istvan Enyedy, and Ildiko M. Kovach*

Department of Chemistry, The Catholic University of America, Washington, D.C. 20064

Received January 24, 1995; Revised Manuscript Received April 24, 1995⊗

ABSTRACT: Molecular mechanics and dynamics combined with semiempirical calculations were carried out for purposes of comparison of the active site characteristics of AChE,[1] trypsin, and chymotrypsin as probed by their diastereomeric adducts with 2-(3,3-dimethylbutyl) methylphosphonofluoridate (soman), methylphosphonate monoester anions, and tetravalent carbonyl intermediates of the reactions of the natural substrates in each case. Glu199 is a key residue in the electrostatic catalytic mechanism of AChE, in removal of the leaving group, and possibly by acting as an alternate general base catalyst. "Pushing" of an alkoxy ligand by Glu199 and the numerous small van der Waals interactions promote dealkylation in phosphonate adducts of AChE much more effectively than any other enzyme. A high concentration of negative charge created by the phosphonate ester monoanion and Glu199 adjacent to it fully accounts for the resistance to the attack of even the strongest nucleophile applied for enzyme reactivation. Stabilization of the developing negative charge on the phosphonates in the soman-inhibited P_SC_S adducts of serine hydrolases is by electrophilic residues in the oxyanion hole (AChE) and the protonated catalytic His. P_R diastereomers of soman-inhibited AChE can be accommodated in an orientation in which the oxyanion hole interactions are lost and for which the stabilizing interactions are 17−26 kcal/mol smaller than in the P_S diastereomer.[2] The dealkylation reaction is almost equally likely in all diastereomers of soman-inhibited AChE. The stabilizing interaction energies are ~4 kcal/mol greater in the P_R than in the P_S adducts of the soman-inhibited serine proteases. There is 0.60 unit greater partial negative charge on the phosphonyl fragment in the anion of phosphonate monoesters of Ser than at the oxygens of tetravalent carbonyl transients resulting in ~12−22 kcal/mol greater stabilization of the former than the latter.

Acute toxicity of organophosphorus compounds (OP)[1] is predicated on their action on AChE (Johnson, 1980; Quinn, 1987; Quinn et al., 1991) which regulates the concentration of the neurotransmitter acetylcholine (Main, 1979; Rozenberry, 1975). Inhibition of other serine hydrolases also causes some serious physiological impairments that have not yet been characterized in detail (Johnson, 1980). Moreover, tetravalent phosphate and phosphonate adducts formed with the active site Ser of serine hydrolase enzymes have been considered "transition state analogs" (Lienhardt, 1973) for acylation and deacylation of the enzymes in the reaction with the natural substrates (Kovach, 1988a,b). As such, they have become probes of the structural features of enzyme active sites in the course of catalysis.

Serine hydrolases are remarkable catalysts owing to a unique combination of catalytic features composed of the catalytic triad (Ser, His, Glu/Asp), the oxyanion hole, and the specificity binding site (Blow et al., 1969; Polgar, 1987; Sussman et al., 1991). While the latter may vary significantly among the members of this large class of enzymes, they all perform the task of nucleophilic displacement at carbonyl by a double displacement mechanism, shown in eq 1, involving two proton-transfer steps in each phase (Blow et al., 1969; Polgar, 1987).

$$\begin{aligned} \mathrm{SerOH + RCOX \rightarrow SerOCOR + XH} \quad &\text{acylation} \\ \mathrm{SerOCOR + H_2O \rightarrow SerOH + RCOOH} \quad &\text{deacylation} \end{aligned} \tag{1}$$

One point of interest in the elucidation of the mechanisms of action of these enzymes has been the kinetic significance of the proton-transfer steps and the mode in which they participate in the bond-breaking and -making steps. A major contribution to the understanding of how serine hydrolases use protolytic catalysis came from the implementation of the proton inventory technique (Venkatasubban & Schowen, 1987). These studies have shown that proton removal from the catalytic Ser by the His is enforced by a compression of

† Supported by the National Science Foundation through Grant MCB9205927 and in part by the U.S. Army Medical Research and Development Command through Contract DAMD-17-C-1064.

‡ On leave from the Central Research Institute for Chemistry of the Hungarian Academy of Sciences, P.O. Box 17, H-1525 Budapest, Hungary.

⊗ Abstract published in *Advance ACS Abstracts,* July 1, 1995.

[1] Abbreviations: AChE, acetylcholinesterase (acetylcholine acetylhydrolase); CSD, Cambridge Structural Database; HI6, 1-[2-[(hydroxyimino)methyl]-1-pyridino]-3-[4-[(hydroxyimino)methyl]-1-pyridino]-2-oxapropane dichloride; Hip, protonated His; INH, inhibitor; OP, organophosphorus compounds; MNDO, minimum neglect of differential overlap; soman, 2-(3,3-dimethylbutyl) methylphosphonofluoridate; sarin, 2-propyl methylphosphonofluoridate; THI, tetrahedral intermediate.

[2] All interaction energies were calculated under completely identical conditions with the same number of solvate water for each enzyme. The protein−protein interactions were essentially unchanged from structure to structure, and water−water and protein−water interactions varied very little. Thus, the differences in interaction energies were completely related to the interactions of the fragment with the protein and water environment. Although calculation of free energy perturbation may be considered the most rigorous method of evaluation of relative stabilities of the adducts, the structures compared in this work are structural isomers or close analogs which should lend credence to the data analysis.

0006-2960/95/0434-8989$09.00/0

the closed active site region. The extent of this compression of the distance between acid/base catalytic residues depends on the intensity of subsite interactions between protease and protein or peptide substrate. The compression is manifest in the number of protons participating in the reaction coordinate motion, between potential donors and acceptors such as Nϵ of His57 and the OH of Ser195 and Nδ-H of His57 and β-COO$^-$ of Asp102 in trypsin, in the rate-determining step(s) and the magnitude of the fractionation factors. A very similar proposition for the compression of bonds at the transition state was put forth recently to explain the occurrence of low-barrier hydrogen bonds (strong H-bonds) between Nδ-H of His57 and β-COO$^-$ of Asp102 which stabilize the quasitetrahedral transition state in the course of acylation of chymotrypsin (Frey et al., 1994). The postulate was based on new NMR measurements on the low-frequency chemical shift involving the Nδ-H(D)---O bond at pH ~3.0 (protonated His) and in transition-state analogs. The Nδ-H(D)---O distance between His57 and Asp102 extracted from these measurements is <2.6 Å, characteristic of a strong H-bond (>12 kcal/mol).

Only single-proton participation was observed in AChE catalysis of the hydrolysis of a number of substrates (Kovach et al., 1986a; Quinn, 1987). This may be a point worth of contemplation, in view of the exceptional catalytic efficiency of AChE, extolled recently (Quinn et al., 1991; Sussman et al., 1991; Gilson et al., 1994; Ripoll et al., 1993; Tan et al., 1993). We have in the past proposed the need for strong electrostatic and hydrophobic interactions for poising and distorting the small substrate, acetylcholine, which does not provide the leverage peptides do for lowering the transition-state energy for hydrolysis (Kovach, 1988a,b). The acid/base catalytic power appears to stem from a different contribution of the catalytic triad and the oxyanion hole in AChE.

The molecular origins of inhibition of serine hydrolase enzymes by phosphonate esters, outlined in eq 2, have been

$$\text{SerOH} + \text{RR'OP(O)X} \rightarrow \text{SerOP(O)ROR'} + \text{XH} \quad \text{phosphonylation}$$

$$\text{SerOP(O)ROR'} + \text{H}_2\text{O} \rightarrow \text{SerOH} + \text{RR'OP(O)OH} \quad \text{dephosphonylation} \quad (2)$$

investigated extensively in this laboratory (Kovach et al., 1986b, 1988; Kovach, 1988a,b; Kovach & Schowen, 1987; Bennet et al., 1988, 1989). A remarkable efficiency (60–70%) of mobilization of the catalytic power of these enzymes was observed in the P–O bond formation at the active site Ser in some cases (Kovach et al., 1986b; Kovach, 1988a,b). Small phosphonate esters use protolytic catalysis provided by the enzyme as unnatural acyl substrates do (Kovach et al., 1986b, 1988). We have also found that the catalytic assistance is diminished or absent in the dephosphonylation of the enzymes which account for their often irreversible inhibition and ensuing toxicity.

The major differences between the reactions of substrate and phosphonates/phosphates catalyzed by AChE are (1) there is the negligible leaving group dependence of the former versus the large leaving group dependence of the latter, (2) there is the smaller stability of the acetyl-enzyme than that of the phosphoryl-enzyme, and (3) the barrier for deacetylation is greatly reduced with respect to the non-enzymic reference, while the barrier for dephosphorylation approaches that for the nonenzymic reaction (Kovach, 1988a). The differences in leaving group effects between acylation and phosphorylation of AChE reflect on structural differences at the transition states, which must be inherent in the differences in the electronic makeup of carbon and phosphorus. Most of these tenets are valid for the inhibition of other serine hydrolases by OPs.

The worst aspect of OP inhibition of serine hydrolases is the occurrence of an irreversible side reaction resulting in the formation of a negatively charged monoester between Ser and phosphonate (diester of a phosphate) (Aldridge & Reiner, 1972; Barnard, 1974). An intensely studied version of this aging reaction is dealkylation involving S_N1 or S_N2 displacement at the Cα of an alkyl group of the phosphonate/phosphate ester of Ser. There is no parallel to the efficiency of the dealkylation reaction occurring in soman-inhibited AChE. It has been shown to occur with the intervention of a carbonium ion, which rearranges to alkene products faster than it is captured by water (Smith & Usdin, 1966; Michael et al., 1967). Phenolic ester linkages, on the other hand, undergo nucleophilic displacements at P (Bender & Wedler, 1972). Different enzymes promote each process differently, presumably, according to the electronic and spacial characteristics of the active site. We have been most interested in elucidating the promotion of each of these reactions (eq 3) by specific active site motifs to learn more about the diversity of serine hydrolase catalysis.

$$\text{SerOP(O)ROR'} + \text{H}_3\text{O}^+ \rightarrow \text{SerOP(O)ROH} + \text{R'}^+ + \text{H}_2\text{O}$$

$$\text{SerOP(O)ROAr} + 2\text{H}_2\text{O} \rightarrow \text{SerOP(O)RO}^- + \text{ArOH} + \text{H}_3\text{O}^+ \quad (3)$$

Serine hydrolase enzymes also show a remarkable selectivity toward chiral phosphonate esters which can be exploited to probe the steric requirements at the active site of the enzymes. To understand the charge distribution on tetravalent neutral serine esters of phosphates, phosphonates, their anionic monoesters and the corresponding carbonyl transients, we have in the past calculated these with MNDO (Kovach & Huhta, 1991). A comparative analysis showed a significantly greater amount of negative charge accumulation on the oxygens of phosphate and phosphonate esters than on the comparable tetravalent intermediates of carbonyl reactions. No doubt that the accumulation of charge should be still less at the quasitetrahedral transition states. The question then emerges: to what extent are these tetravalent adducts good in mimicking transition states and what can one learn from using them as probes of the active site of enzymes?

The structural perspective of these reactions has also been expanded recently as the X-ray crystallographic coordinates of AChE *Torpedo californica*, and a number of conjugates with inhibitors have become available (Sussman et al., 1991; Cygler et al., 1993; Gilson et al., 1994; Ripoll et al., 1993; Tan et al., 1993, Nair et al., 1994). In addition, there is a wealth of structural data to aid characterization of other serine protease reactions. For the thesis of our paper, also valuable are the results of crystallographic and NMR measurements involving OP adducts of AChE (Segall et al., 1993), trypsin

(Adebodun & Jordan, 1989), chymotrypsin (Gorenstein et al., 1989; Grunwald et al., 1989, Kovach et al., 1993; Van der Drift et al., 1985), and other serine hydrolase enzymes (Adebodun & Jordan, 1989, Van der Drift et al., 1985). However, no structural information on the rapidly aging phosphonate ester adducts of Ser at the active site of the enzymes, much less on intermediates with very short life times, can be expected to be forthcoming. We have, therefore, carried out molecular dynamics simulations on the native enzymes and molecular mechanics combined with semiempirical calculations of the Ser−OP conjugate structures. Then, we have undertaken an extensive analysis of energy-minimized structures of diastereomers of soman-inhibited AChE, trypsin, and chymotrypsin adducts. We have compared the minimized structures of the dealkylated diastereomeric adducts and also the tetrahedral transients of carbonyl compounds. We focused attention on the availability of the acid/base catalytic apparatus of the triad, the role of the oxyanion hole, stabilization by the protein of the negative charge at P, the vicinity of an electron-rich residue to stabilize the incipient carbonium ion, and the availability of nonpolar residues at the binding site to facilitate dealkylation. Here we wish to shed light to the general question of how good analogs of transients in the reactions of the three enzymes are the tetravalent phosphonate adducts. Our specific interests are also in the origin of stereoselectivity in phosphonylation of the enzymes and what motivates dealkylation in the phosphonyl adducts of the three enzymes.

EXPERIMENTAL PROCEDURES

The molecular mechanics-optimized structure reported earlier (Qian & Kovach, 1993; Kovach et al., 1994) for AChE was used in these calculations. Trypsin and chymotrypsin were optimized in an identical manner (Zhao et al., 1994). Hydrogen positions on the heteroatoms were assigned and oriented by the programs HYDPOS and ORIENT utilities in molecular mechanics program YETI 5.3 (Vedani, 1990). Both nitrogens Nϵ and Nδ were protonated on the catalytic His. The hydroxyl H-atoms were oriented to match the torsional angles (within 20°) of the neutron diffraction refinement of the monoisopropyl phosphate adduct of Ser in trypsin (Kossiakoff & Spencer, 1981) or were set to the best theoretical angle.

Fragments with Tetravalent Phosphorus. The geometry of the methyl fragment on phosphorus was obtained from a search of the Cambridge Structural Database (CSD) (Allen et al., 1979) of alkyl phosphonyl fragments. The average P−C bond length was 1.81 ± 0.03 Å, the average O−P−C bond angle was 108.707 ± 4.174°, and the average O−P−O bond angle was 105.632 ± 3.086°. These values agreed with the values generated with MNDO within 1%.

Refinement of the Covalent Adducts of Enzymes. For the atom-centered charge calculations, a tripeptide built from the enzyme active site and its adjacent residues (194−196 for serine proteases) was used. The active site Ser was covalently modified with the desired fragment. The structures were then refined with the MNDO method as implemented in MOPAC 6.0 (Dewar et al., 1985), optimizing the side chain and all hydrogen atom positions only. Tetravalent transients, the methyl acetate adduct of AChE to mimic its reaction with acetylcholine and the acetamide adduct of trypsin and chymotrypsin to mimic their reaction with an amide, were generated in MNDO. The refined structure was then used for the calculation of the electrostatic potential-fit atomic charges. The main-chain NH and CO charges were set to the value used in YETI (Vedani, 1990) for future refinements of the whole protein. Any unbalanced charge was then ameliorated by adjusting the charge on Cα and Cβ by equal amount. Absolute values of the excess charge were only a few hundreds of a charge unit. Each diastereomer of the serine ester of the appropriate alkoxy alkylphosphonate was then incorporated into the structure of the enzyme to be studied, and the entire structure was again energy-minimized. The same protocol was applied to the tetravalent carbonyl transients.

The refinements were accomplished with the molecular mechanics program YETI. Optimization in YETI is carried out in an internal/Cartesian coordinate space with a conjugate-gradient minimizer. All the bond lengths and bond angles and all the positions of main-chain atoms are kept constant during calculation. The YETI force field consists of only nonbonded energies: electrostatic, H-bonding, van der Waals, metal−ligand, and torsional energy terms. Electrostatic energies were calculated with the distance-dependent dielectric parameter set to $D(r) = 2.0r$ (Jorgensen et al., 1983; Singh et al., 1986) based on the experience of Vedani (1990) with similar systems. The cutoff criteria were as follows: 9.5/10.0 Å for electrostatic interactions, 6.5/7.0 Å for van der Waals interactions, and 4.5/5.0 Å for H-bonding interactions. Convergence criteria were set to 0.025 kcal mol^{-1} deg^{-1} for the torsional RMS first derivative, to 0.025 kcal mol^{-1} deg^{-1} for the rotational RMS first derivative, and to 0.250 kcal mol^{-1} Å^{-1} for the translational RMS first derivative. The energy convergence criterion was ±0.05 kcal mol^{-1}. Low-energy conformations were identified by searching the conformational space around the torsional angle Cβ−Cγ for the catalytic His, around all dihedral angles in the phosphonyl fragment, and the oxyanion hole region in each enzyme.

Molecular dynamics simulations were carried out with program CHARMM (version c22g5) (Brooks et al., 1983) on energy-minimized native AChE and trypsin solvated with one water shell to probe the mobility of the catalytic His and components of the oxyanion hole. All atoms were represented explicitly. The TIP3P model, as implemented in CHARMM, was employed for the simulation of solvate water molecules. The parameters for the amino acid residues were from the standard parameter file of the CHARMM program. No H-bonding term was used in the empirical potential energy function. Numerical integration by the leap frog integrator with a 1 fs step size was used for the molecular dynamics calculations. A switching function was used on the force for the long-range nonbonding energy terms with the cutoff value of 12 Å.

The temperature of the energy-minimized system was raised from 50 to 300 K in 5 K steps in every 0.5 ps and then equilibrated for 5 ps with or 10 ps without velocity adjustment. The coordinates were saved at every 0.2 ps for later analysis in 120 ps production runs.

Program GEMM (V7.87; Cammissa et al., 1992) was used for visualization of the structures. The calculations were carried out on an SGI Personal Iris 4D35 and an Indigo^2 workstation and on a cluster of HP-735 workstations.

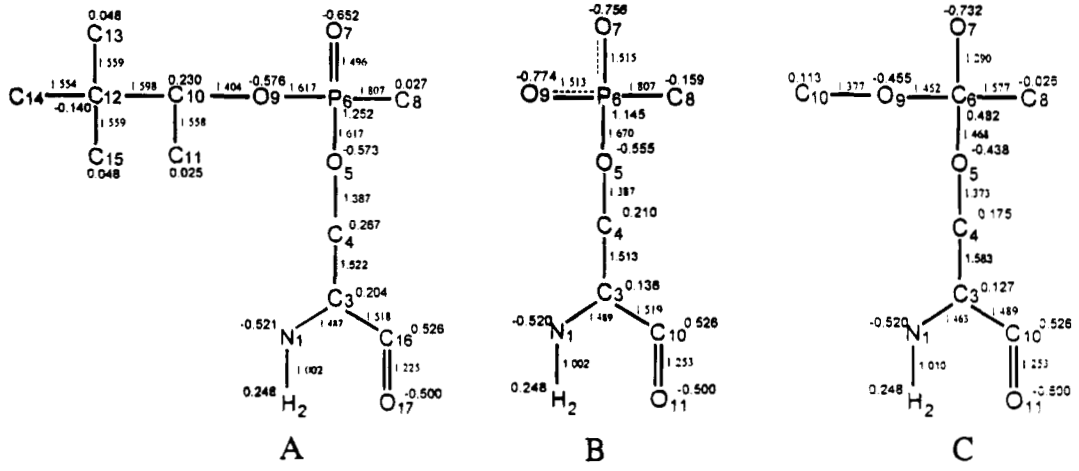

FIGURE 1: Connectivity and partial atomic charges for three tetrahedral adduct fragments of the active site Ser of a serine hydrolase with (A) soman, (B) the product of dealkylation of soman, and (C) methyl acetate. Hydrogens are not shown, and their charges are added to that of the heavy atom bonded to them.

RESULTS

Molecular mechanics calculations were performed with the fully solvated structures of AChE from *T. californica* (556 water molecules), bovine trypsin (383 water molecules), and bovine γ-chymotrypsin (460 $\pm$ 5 water molecules). For the molecular dynamics simulations, the enzymes were fully solvated with an ~5 Å water layer. Molecular mechanics calculations were also carried out on the *diasteromers* of the tetravalent adducts of each soman-inhibited enzyme and the products of dealkylation, the diasteromeric tetravalent monoester phosphonate adducts. The tetrahedral adducts formed with carbonyl compounds, methyl acetate, acetic acid, and acetamide, were also studied for purposes of comparison of the mechanisms of catalysis of the two groups of enzymes. Figure 1 shows a representative comparison of the charge distribution on the pinacolyl methylphosphonate ester of Ser, the corresponding dealkylated adduct, and a tetrahedral carbonyl intermediate occurring in the AChE-catalyzed reaction of an ester. These geometry-optimized fragments with charges were then incorporated into the proteins; the adducts were fully solvated and energy-minimized.

The active site interactions with the pinacolyl methylphosphonyl fragments in the adducts with P_SC_S configuration are shown in Figure 2 for AChE, in Figure 3 for trypsin and in Figure 4 for chymotrypsin. Figures 5 and 6 show the interactions in the corresponding adducts of AChE and trypsin, but with P_RC_S configuration. Figures 7 and 8 show the structures of the dealkylated methylphosphonate anion adducts with P_S configuration for AChE and trypsin, respectively, and Figure 9 shows the same with P_R configuration for trypsin. The tetrahedral adduct of methyl acetate with AChE is shown on Figure 10, and two possible orientations for tetrahedral adducts formed between trypsin and acetamide are displayed in Figures 11 and 12. The former corresponds to a transient formed immediately after His-catalyzed attack of Ser at a peptide bond to an L-amino acid. Analogous structures were also computed for chymotrypsin but not shown. The geometric parameters for critical interactions are in Tables 1–3, and a comparison of the sum of critical interactions between protein–fragment, fragment–fragment, and water–fragment is shown in Table 4. Protein–protein interactions were within 5 kcal/mol for each adduct of an enzyme, and protein–water interactions were within 100 kcal/mol, corresponding to no more than a difference of 2–8 water molecules. The values of protein–fragment, water–fragment, and fragment–fragment interaction energies were insensitive to differences of even 70 water molecules in the solvent shell between structures.

DISCUSSION

Comparison of the Charge Distribution in the Tetravalent Ser Adducts (Figure 1). Whereas the geometries of phosphonates and the tetravalent transients of carbonyl compounds are very similar, the charge accumulation on the phosphoryl and anionic oxygens in the dealkylated phosphonates are much greater than on the tetravalent intermediate formed in the natural reactions. The overall energy contribution from steric fit at the active site and solvation of tetravalent phosphonates and carbonyl transients is nearly equal in the neutral adducts, while the dominant interaction energies are electrostatic in the anionic phosphonate monoester adducts of the enzymes. In fact, stabilizing energies in the anionic phosphonate ester adducts of serine hydrolases are by 7–16 kcal/mol greater than those in the tetrahedral intermediates in the reactions of small esters and amides (Table 4). No doubt that transition states preceding or succeeding the covalent intermediates in acylation and deacylation of AChE have even smaller polarization and therefore bear less resemblance to the charge distribution in phosphonate ester anions. These differences in charge distribution present a limitation to the use of anionic phosphonate esters as "transition state analogs".

In addition to the accumulation of strong negative charge on the aged adduct in AChE, Glu199 in the vicinity further militates against the odds for successful nucleophilic displacement at P and ensuing regeneration of enzyme activity. The phosphonyl fragment is surrounded by the oxyanion hole which blocks access on one side and Glu199 providing additional negative charge borders it on the other side. This problem is plaguing whether solvation of the charge occurs or not. If a solvate chain replaces the alkyl moiety, it is difficult to penetrate. If the active site is dry, then the low dielectric field enhances the effect of the local negative charge around P.

Stereochemistry of Phosphonylation. Phosphonylation of the active site Ser by the P_S diastereomers of soman is >1000

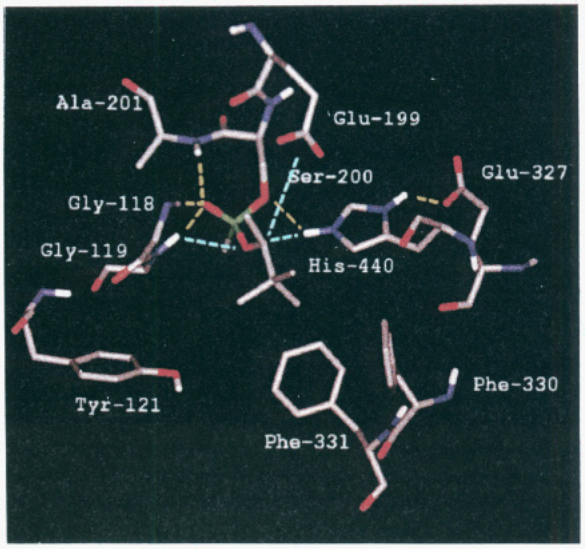

FIGURE 2: Stereochemical relationships at the active site of P_SC_S soman-inhibited *T. californica* AChE. The yellow dashed lines show potential H-bonding interactions in the oxyanion hole and in the catalytic triad, while the blue dashed lines indicate forces promoting dealkylation and elimination of a leaving group.

times faster for AChE and ~100 times faster for trypsin and chymotrypsin than the P_R diastereomers (Broomfield et al., 1984; de Jong & Benchop, 1988). Chirality at the Cα of the pinacolyl side chain has a small effect on the rate of phosphonylation in each case, the C_R configuration being more favorable (de Jong & Benchop, 1988).

The stereochemical outcome of phosphonylation of the active site Ser of the serine hydrolase enzymes has not been established with certainty. It is generally assumed that the reaction proceeds with a simple in-line displacement at P with the incursion of a trigonal-bipyramidal transient of structure-dependent lifetime and resulting in inversion of configuration as shown in eq 4 (Westheimer, 1968). It is

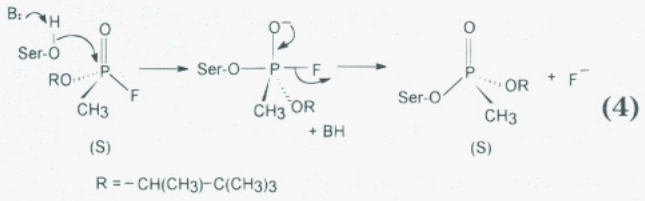

(4)

quite likely that this assumption will hold because only in very rare cases has adjacent attack, in the equatorial plane of a trigonal bipyramid, been proposed (Buchwald et al., 1982). The possibility for perturbational isomerization has also been considered quite remote in phosphonate chemistry (Frank & Usher, 1967; Kovach et al., 1993; Zhao et al., 1994). If expecting simple inversion of configuration in the phosphonylation of the active site Ser as shown in eq 4, the diastereomer of soman, with *S* configuration at P and *S* at C, would give the structures represented in Figures 2–4. Due to a change in the Cahn–Ingold–Prelog priority order of the substituents in P, the notation in the adduct is still P_S after inversion of configuration. In an earlier work, we generated both the P_SC_S and P_SC_R diastereomers of the soman-inhibited AChE (Qian & Kovach, 1993). The accommodation of the pinacolyl group is equally favorable in the diastereomers. The only difference we have observed in the active site conformation is around Hip440. The imidazole side chain of Hip440 is rotated out of the original

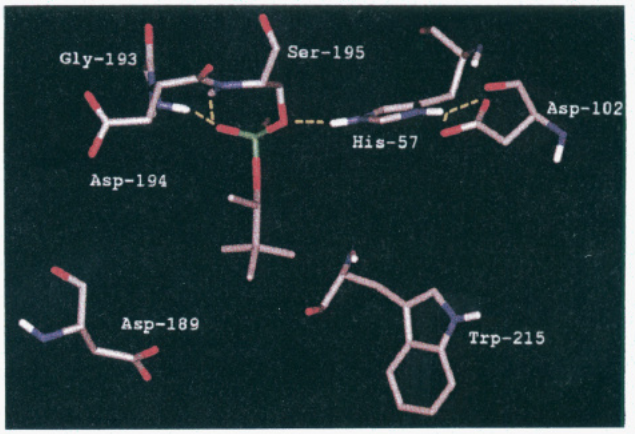

FIGURE 3: Stereochemical relationships at the active site of P_SC_S soman-inhibited trypsin. The yellow dashed lines indicate potential H-bonding interactions in the oxyanion hole and in the active site.

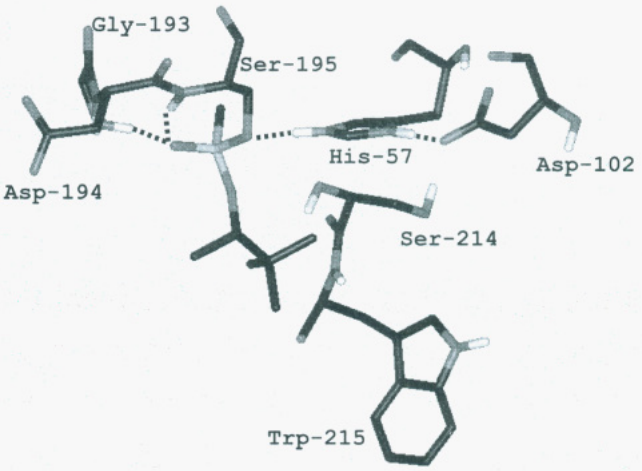

FIGURE 4: Stereochemical relationships at the active site of P_SC_S soman-inhibited chymotrypsin. Dashed lines indicate potential H-bonding interactions at the active site.

conformation in the P_SC_R adduct due to a steric clash with the methyl group facing Hip440. Hip440 then is no longer in alignment with the Oγ of Ser200 for proton transfer. The experimental observations that the rates of dealkylation from the two adducts are almost the same and that the reactivation by oximes (such as HI6) is slower and less efficient from the diastereomer expected to have the P_SC_R configuration are consistent with the results of these calculations (Bencsura et al., 1994).

Key Interactions with the Pinacolyl Methylphosphonyl Fragments in the P_SC_S Diastereomers at the Active Site of the Three Enzymes (Figures 2–4 and Tables 1–3). We wish to emphasize only similarities and differences in geometries and energies of interactions. The absolute values of energies depend on the algorithm and on the value chosen for the distance-dependent dielectric constant (Kovach, 1988b; Kovach et al., 1991). An optimal value of $D(r) = 2.0\tau$ was used in these calculations (Vedani, 1990).

Glu327 holds His440 in the catalytically competent position with a strong electrostatic force at 2.6 Å. The interaction may also be considered a short and strong H-bond with a low (or no) barrier in a double minimum potential energy well (Frey et al., 1994). The unusual feature of the AChE structure is that the short distance is there in the reactant state, although this observation should be interpreted in the context of the error limits of the atomic positions from

Table 1: Distances (Å) and Angles (deg, in Parentheses) in Key Interactions at the Active Site of AChE Covalently Modified with Diastereomers of Soman, the Dealkylated (Aged) Derivative, and Methyl Acetate

interaction[a]	P_SC_S	P_S-aged	P_RC_S	THI[b]
His440Nϵ-H---OESer200	2.92	2.88	2.77	3.15
	(134)	(161)	(127)	(138)
His440Nδ-H---O2Glu327[c]	2.63	2.60	2.59	2.65
	(138)	(142)	(129)	(137)
His440Nϵ-H---OEP	3.61	3.89	4.34	3.80
(OR leaving group)	(150)	(145)	(139)	(163)
INHCα---O2Glu199	4.09		4.82	
INHCα---O2Glu327	8.16		9.38	
Gly118N-H---OPP	2.92	3.05		2.95
(or $^-$OC-carbonyl)	(168)	(174)		(154)
Gly119N-H---OPP	2.77	2.63	4.76	2.69
(or $^-$OC-carbonyl)	(161)	(149)	(121)	(174)
Ala201N-H---OPP	2.69	2.64		2.60
(or $^-$OC-carbonyl)	(120)	(112)		(116)
INHOEP---Gly118N-H	4.07	4.02		3.92
INHC3---hydrophobic residues[d]	3.5−5		3.1−4.5	
WAT950O---OPP		3.88		
WAT950O---O$^-$		2.71		

[a] The pinacolyl, O$^-$, and methoxy groups occupy the binding site for choline; OP = phosphoryl; OE = ester linkage or O$^-$ in dealkylated (aged) adduct; C3 = Cα in pinacolyl. [b] THI mimicking the tetrahedral transient in the reaction of acetylcholine. [c] Strong H-bonds. [d] Tyr121, Tyr84, Phe330, Phe331, Tyr130.

Table 2: Distances (Å) and Angles (deg, in Parentheses) in Key Interactions at the Active Site of Trypsin Covalently Modified with Diastereomers of Soman, the Dealkylated (Aged) Derivative, and Acetamide

interaction[a]	P_SC_S	P_S-aged	P_RC_S	P_R-aged	THI
His57Nϵ-H---OESer195	3.11	3.02	3.05	2.89	3.07
	(132)	(133)	(120)	(121)	(136)
His57Nδ-H---O2Asp102	2.68	2.67	2.76	2.74	2.70
	(148)	(145)	(160)	(151)	(149)
His57Nϵ-H---OEP	4.09	4.10	3.11	2.96	3.52
(NH_2 leaving group)	(163)	(162)	(166)	(164)	(149)
INHCα---O2Asp194	7.68		9.36		
INHCα---O2Asp102	8.03		8.74		
INHCα---O2Asp189	9.20		12.72		
Gly193N-H---OPP	2.68	2.67	2.79	2.88	2.70
(or $^-$OC-carbonyl)	(144)	(140)	(155)	(166)	(143)
Ser195N-H---OPP	2.71	2.77	2.76	3.19	2.71
(or $^-$OC-carbonyl)	(151)	(150)	(148)	(145)	(143)
WAT702O---O$^-$		2.67		2.75	
		(160)		(169)	
WAT710O---O$^-$		2.68			
		(172)			

[a] The pinacolyl and O$^-$ groups in the P_S diastereomers occupy the specificity pocket and those in the P_R diastereomers and the NH_2 in THI face Hip57. Other notations are the same as in Table 1.

Table 3: Distances (Å) and Angles (deg, in Parentheses) in Key Interactions at the Active Site of Chymotrypsin by Covalently Modified by Diastereomers of Soman, the Dealkylated (Aged) Derivative, and Acetamide

interaction[a]	P_SC_S	P_S-aged	P_RC_S	P_R-aged	THI
His57Nϵ-H---OESer195	2.98	2.84	2.91	2.79	2.92
	(127)	(130)	(117)	(120)	(133)
His57Nδ-H---O2Asp102	2.79	2.79	2.85	2.85	2.79
	(169)	(168)	(174)	(173)	(168)
His57Nϵ-H---OEP	3.59	3.40	2.96	2.86	3.83
(NH_2 leaving group)	(141)	(138)	(167)	(160)	(141)
INHCα---O2Asp194	8.12		9.10		
INHCα---O2Asp102	7.69		8.71		
Gly193N-H---OPP	2.65	2.63	2.79	2.75	2.67
(or $^-$OC-carbonyl)	(137)	(136)	(144)	(146)	(139)
Ser195N-H---OPP	2.79	2.94	2.71	2.99	2.81
(or $^-$OC-carbonyl)	(155)	(155)	(149)	(152)	(154)
WAT702O---O$^-$		2.70		4.32	
		(177)		(140)	

[a] The pinacolyl and O$^-$ groups in the P_S diastereomers occupy the specificity pocket and those in the P_R diastereomers and the NH_2 in THI face Hip57. Other notations are the same as in Table 1.

the X-ray diffraction data (2.2 Å resolution). If a short H-bond is already present, then further tightening of the Glu327 β-COO$^-$−His440 Nδ distance at the transition state may not result in lowering the energy and there will not be an observable participation of the proton in the reaction coordinate motion. This is in fact supported by the linear proton inventories for the AChE reactions indicating the motion of a single proton, most likely the one transferring from Ser200 to His440 (Kovach et al., 1988). What is then the function of this strong H-bond or salt bridge? It anchors the His by restricting the torsional rotation along the Cβ−Cγ bond in the resting state and thereby keeping the lone pair electrons on Nϵ of His440 poised for removal of the proton from Ser200.

In contrast, the Asp102 β-COO$^-$−His57 Nδ distance is 0.2−0.3 Å longer in the resting state in the serine proteases, but covalent modification of the Ser causes a shortening of the distances between H-bond donors and acceptors at the active site by 0.1−0.2 Å. These differences are observable in the X-ray structures of the native and covalently modified serine proteases (Chambers & Stroud, 1977) by NMR measurements (Frey, 1994; Bachovchin, 1986), and are also consistent with the proton inventory results (Venkatasubban & Schowen, 1987).

Although early mechanistic investigations implicated the *involvement of the protonated catalytic His* in the dealkylation process (Michael et al., 1967; Berman & Decker, 1986; Schoene et al., 1980), these calculations cast doubt on this assumption. Electrostatic and H-bonding interactions in the P_SC_S adducts are somewhat stronger between the catalytic Hip and Ser Oγ than with the ester O in the OR′ fragment (eq 2) in the minimum energy conformation of each adduct. This former orientation was called the "in" position by Bizozero and Dutler (1986; Nakagawa et al., 1993) and corresponds to the first phase of the reactions of substrates and inhibitors, *i.e.*, the His-catalyzed nucleophilic attack by Ser. The latter orientation corresponds to the "out" position and corresponds to the protonation of the leaving group in the substrate reaction. Furthermore, the interaction between Hip440 Nϵ and OEP is stronger in the P_S diastereomers of the soman-inhibited AChE than in the P_R adducts. This is due to the stronger van der Waals interactions between the pinacolyl group and hydrophobic residues of the active site in the P_S than in the P_R adducts that apparently pulls the active site components closer. The Hip440 Nϵ−OC distance in the tetrahedral intermediate with methyl acetate is just 0.2 Å longer than in the P_S adducts, in accord with the smaller interaction between the methyl group and the hydrophobic residues.

In native AChE, the average distance between the Oγ of Ser200 and Nϵ of His440 was 2.8 Å during a 120 ps molecular dynamics simulation. In contrast, a similar simulation showed an average distance of 4.0 Å, with a 5−15 ps time span at ~3.0 Å between Oγ of Ser195 and Nϵ of His57 in native trypsin. We have also evaluated the conformational mobility of the catalytic His at the active site

in the native enzymes by molecular dynamics and in the adducts by molecular mechanics. All showed a single minimum conformation. It was particularly critical to ascertain this fact, because in our earlier molecular mechanics calculation involving two soman−AChE diastereomers, we had observed that the methyl group in Cα is in steric conflict with the imidazole side chain of Hip440 in the P_SC_R diastereomer (Qian & Kovach, 1993). This caused a 60° rotation of the ring around the Cβ−Cγ bond and placed the protons on Hip440 out of alignment for optimal proton transfer to Ser200. Without protonation the Ser is a poor leaving group, and enzyme reactivation should be inhibited. This has in fact been observed for the diastereomer believed to have the P_SC_R configuration. This catalytically unproductive conformation had a very short residence time in a 120 ps simulation of the dynamics of the native enzyme. However, conformational mobility of the catalytic His in the native and modified enzymes may be different as was the case for acylchymotrypsin (Nakagawa et al., 1993).

Although Nε of Hip440 is 3.6 Å away from the alkoxy oxygen in the pinacolyl group, a hemisphere of H-bond donors that constitute the oxyanion hole (Gly119) wraps around the phosphonyl fragment from the "west side" on Figure 2. All of these electrostatic and H-bonding forces should have a stabilizing effect on the developing negative charge on the oxygen during C−O bond cleavage. Indeed, pH−rate profiles of the dealkylation in soman-inhibited AChE show a maximum around pH 6, but the rates continue to decrease with a slope close to 1 up to pH 10 (Viragh et al., unpublished results). This finding is not consistent with protolytic catalysis by a protonated His alone unless its pK is above 10, which would be surprising at the least.

The oxyanion hole interaction is very strong in the P_SC_S diastereomer of the soman-inhibited AChE. Gly118 and Gly119, which come from a part of the chain remote from Ser200, are very strong H-bond donors, and Ala201 provides a weak interaction to stabilize the oxyanion of the tetrahedral intermediate or the phosphoryl group. The three H-bond donors form a hemisphere of positive electrostatic environment whereas there are only two H-bonds in the serine proteases. The location of the oxyanion hole in the two groups of enzymes is also the opposite with respect to the backbone.

The pinacolyl group is stabilized by small *nonspecific van der Waals interactions* in the binding region of the natural substrate in each case. Tyr121, Tyr84, Phe330, and Phe331 are within strong van der Waals contact with the pinacolyl group in AChE. A somewhat weaker hydrophobic stabilization, mostly with Trp215, exists in the serine proteases, particularly in trypsin.

The Role of Glu199. Inception of the carbonium ion seems to be promoted by a strong negative electrostatic force. In addition to a global negative electrostatic field, *Glu199 in the local environment of the phosphonyl fragment at the active site of AChE seems to provide the major driving force to the dealkylation reaction.* It is at 4 Å distance from the Cα of the pinacolyl group in the P_SC_S adduct. We have pointed out earlier the critical role of Glu199 in the aging reaction in AChE (Qian & Kovach, 1993). Experimental verification of its key role has since been obtained in substrate reactions of AChE (Selwood et al., 1993) as well as in the dealkylation of soman-inhibited mammalian AChEs. The dealkylation reaction in the soman-inhibited Glu202Gln mutant of human erythrocyte AChE was reduced by 200-fold (Ordentlich et al., 1993) and the Glu199Gln mutant of the *T. californica* AChE by a significant amount (Saxena et al., 1993).

Figure 2 shows how the side chain wraps around the active site with the carboxylic acid coming within 3.5 Å of the Oγ of Ser200. Although a similar conformation in the native state, in which Ser200 may engage in a H-bonding interaction with Glu199, seems to be strained and less prevalent, one may wonder if this orientation has kinetic significance by providing nontraditional general acid/base catalysis in AChE reactions with large substrates. A nontraditional mode of catalysis by AChE was recently observed in the hydrolysis of butyrylthiocholine and benzoylcholine (Selwood et al., 1993). Selwood et al. suggested that Glu199 may act as a general base assisting water attack, instead of Ser attack, at the carbonyl C. However, it seems more likely to us that Glu199 simply acts as a surrogate general base catalyst in proton removal from Ser200 in certain strained conformations. In fact, the soman-inhibited AChE adduct may be considered a good model of butyryl-AChE. Insertion of a water molecule between the phosphonyl moiety and Glu199 would require a considerable motion of active site residues and the phosphonyl fragment away from the optimum structure shown in Figure 2.

Asp194 in the serine proteases is the counterpart of Glu199 in the sequence homology. It is 9−13 Å away from the phosphonyl fragment in each case. The remote location of negatively charged residues from the phosphonyl fragment in the serine proteases is then consistent with the much subdued tendency for dealkylation in these enzymes (Johnson, 1980; Kovach, 1988a). A different orientation of Glu199 from Asp194 indicates that the two amino acids evolved to fulfill different roles. Asp194 plays a critical role in the activation of serine proteases from the zymogen (Polgar, 1987), while similar development has not been observed for AChE. In contrast, Glu199 seems to be a key residue in stabilizing the choline fragment of the natural substrate and in catalyzing the chemical reactions of substrates and inhibitors of AChE. Since carboxylic side chains occur in the amino acids preceding the catalytic nucleophile in both groups of enzymes, it is tempting to speculate that in previous times they served the same purpose (enzyme activation from a zymogen).

Conformation of the P_R Diastereomers of the Pinacolyl Methylphosphonyl Adducts. The phosphonyl group of the P_R adducts of the soman-inhibited AChE cannot be accommodated in the oxyanion hole because it would result in a steric clash of the pinacolyl group with residues of the active site gorge. There is one way for these diastereomers to bind, that is, with the methyl group in the oxyanion hole which results in loss of many stabilizing interactions. In principle, the P_R diastereomers of soman-inhibited AChE would also dealkylate because the location of the pinacolyl group does not change in our model. The Cα of the pinacolyl group is still 4.8 Å away from Glu199, which may "push" the oxyanion out and stabilize the carbonium ion intermediate. The pinacolyl oxygen can also interact with the same positively charged environment as in the other diastereomers. This is clearly indicated in Figure 5. The energy of interaction between the protein and phosphonyl fragment is 16.5 kcal/mol more favorable for the P_SC_S diastereomer of the soman-inhibited AChE than that in the P_RC_S diastereomer.

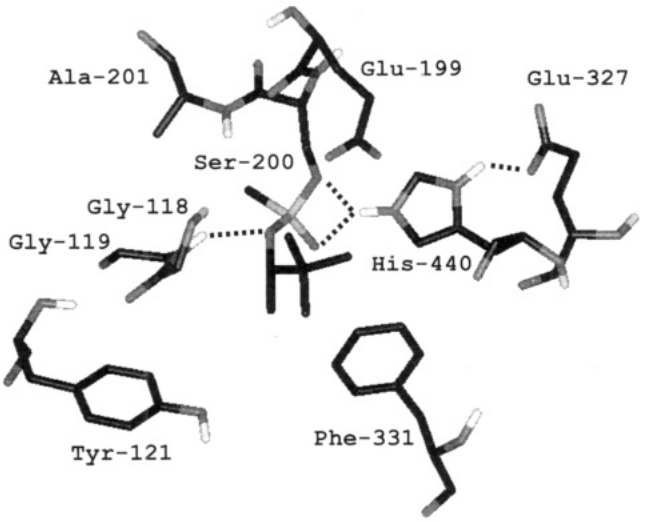

FIGURE 5: Stereochemical relationships at the active site of P_RC_S soman-inhibited *T. californica* AChE. Dashed lines indicate potential H-bonding interactions at the active site.

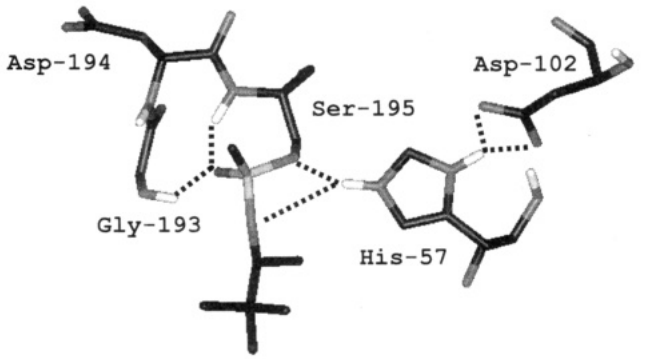

FIGURE 6: Stereochemical relationships at the active site of P_RC_S soman-inhibited trypsin. Dashed lines indicate potential H-bonding interactions at the active site.

An additional ~9 kcal/mol can be obtained from protein−water interactions.

In contrast, the critical oxyanion interaction (~5−8 kcal/mol) can be maintained in all adducts of soman-inhibited serine proteases (Figure 6). The optimum structure of the P_RC_S diastereomer of the pinacolyl methylphosphonyl adducts of these enzymes has the pinacolyl moiety facing the opening of the active site cavity. The hydrophobic alkyl side chain may interact with the so-called "N-acyl binding site", but it encounters some steric crowding with the catalytic Hip. It is also less favored by the bulk solvent than by the specificity pocket as in the P_SC_S diastereomers. Yet, the protein−fragment interactions are more favorable by ~4 kcal/mol in the P_RC_S diastereomers of the soman-inhibited chymotrypsin and trypsin, which is attributable to the better interaction between Hip57 and the OEP in the P_R adducts. This means that in-line displacement at P by Ser195 on P_SC_S soman, the more active diastereomer, would result in the less stable of the soman-inhibited serine protease diastereomers.

The Anionic Methylphosphonate Esters of Ser in AChE, Trypsin, and Chymotrypsin. Dealkylation occurs with extreme facility in the P_SC_S or P_SC_R adducts of soman-inhibited AChE. It is difficult to assess the rate for the other two P_R diastereomers because they are not readily generated (Keier & Wolring, 1969; de Jong & Benchop, 1988). However, all four diastereomers of the cyclohexyl alkylphosphonate adducts of AChE were generated, and their

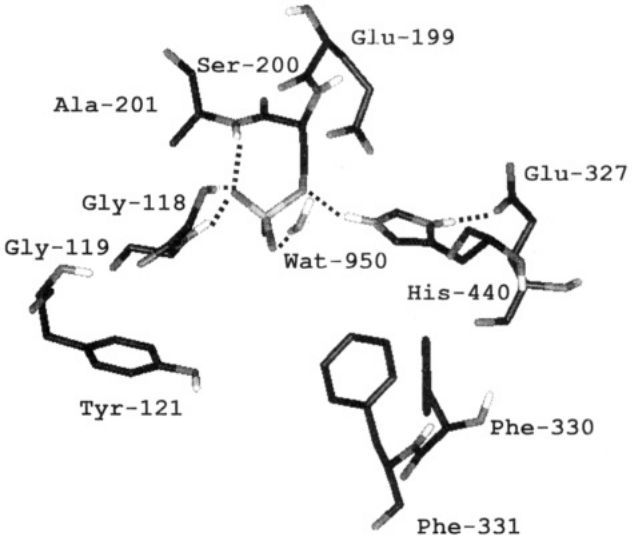

FIGURE 7: Stereochemical relationships at the active site of P_S soman-inhibited *T. californica* AChE after dealkylation. Dashed lines indicate potential H-bonding interactions at the active site.

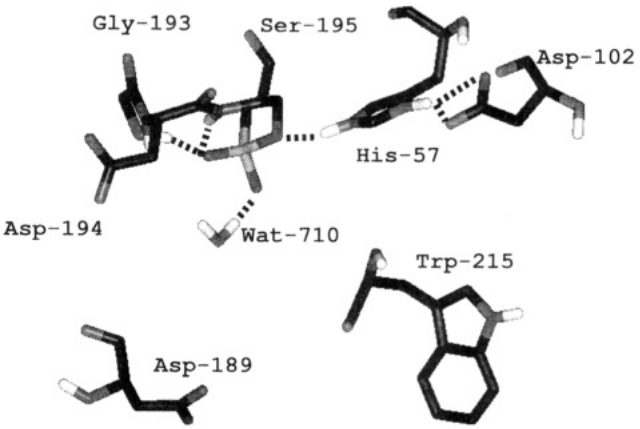

FIGURE 8: Stereochemical relationships at the active site of P_S soman-inhibited trypsin after dealkylation. Dashed lines indicate potential H-bonding interactions at the active site.

facile dealkylation has been reported (Berman, 1994; Berman et al., 1986). Dealkylation in the P_S-soman-inhibited diastereomers of trypsin occurs very slowly (Hartley & Kilby, 1952, 1954; Cohen et al., 1962). The process is essentially unobservable in chymotrypsin (Green & Nicholls, 1959; Segall et al., 1993). Much less information is available about the rates of dealkylation of the P_R-soman-inhibited trypsin or chymotrypsin diastereomers. These are expected to be particularly vulnerable to dealkylation, since the P_R-sarin-inhibited trypsin adducts were studied and dealkylation was observed (Kovach et al., 1993). Presumably, dealkylation does not involve a change in configuration at P, and thus, the structures shown in Figures 7 and 8 would result from the dealkylation of the P_S diastereomers of the pinacolyl methylphosphonyl adducts of AChE and trypsin, respectively. An analogous structure for chymotrypsin, not shown, was also generated.

The anionic charge is stabilized by H-bond donors, Gly119 in particular, of the oxyanion hole residues, Hip440, and two solvate molecules of a chain of water in the AChE active site. In the P_RC_S adduct of soman-inhibited AChE the negative charge remaining on the oxygen after dealkylation is at the same site as in the other diastereomer shown in Figure 7, since the pinacolyl group cannot fit anywhere else.

Table 4: Differences in the Sum of Protein−Fragment (P−F), Water−Fragment (W−F), and Fragment−Fragment (F−F) Interaction Energies (kcal/mol)[a] among Phosphonate and Carbonyl (THI) Adducts of AChE, Trypsin, and Chymotrypsin

adducts compared	P−F	W−F	F−F	total
AChE P_S−P_R	−14.0	0.5	−3.0	−16.5 (−9)[b]
AChE P_S-aged−P_S	2.3	6.5	−2.1	−6.2
AChE P_S-aged−THI	−3.6	−11.0	−1.0	−15.6
trypsin P_S−P_R	−0.4	0.5	−3.0	4.5
trypsin P_S-aged−P_S	−1.8	−16.1	−4.5	−22.4
trypsin P_S-aged−THI	0.8	−21.6	0.0	−20.8
chymotrypsin P_S−P_R	4.0	2.0	−0.7	5.3
chymotrypsin P_S-aged−P_S	−3.0	−18.6	0.0	−21.6
chymotrypsin P_S-aged−THI	0.0	−15.0	3.0	−12.0

[a] Protein−protein interactions were completely balanced for P_S−P_R pairs of diastereomers and were within 5 kcal/mol for all other adducts of an enzyme. The differences in interaction energies were the same within 0.5 kcal/mol for trypsin when the cutoff criterion for electrostatic interactions was set to 10/12 Å. [b] Difference in protein−water and water−water interactions.

The dealkylation reactions in the P_S adducts of soman-inhibited AChE, trypsin, and chymotrypsin are associated with −6.2, −22.4, and −21.6 kcal/mol interaction energy, respectively (Table 4). The stabilizing interaction energy is smaller in the dealkylated P_S diastereomeric adducts of AChE than in the serine proteases, despite the greater number of interactions at the active site, because of the large electrostatic repulsion (~7 kcal/mol) between the COO^- of Glu199 and phosphonyl anion−O^- at a <5 Å distance. Nevertheless, the sum of the electrostatic repulsion must be responsible for deterring the attack of even the strongest nucleophile.

The solvation energy decreases on dealkylation of the soman-inhibited serine protease adducts by ~15 kcal/mol for the P_S adducts and ~5 kcal/mol for the P_R adducts. Dealkylation of the P_S adduct leaves the specificity pocket of the enzymes open to fill with solvent which then surrounds the O^- of the phosphonyl fragment. In contrast, the leaving group binding site, the location of the O^- in the aged P_R adducts, is more shielded from solvent than the specificity pocket, which is the reason for the difference in solvation energy. The protein−phosphonate stabilization energy in trypsin is then very close to the −6 kcal/mol calculated for the same (P_S) diastereomer unsolvated (Kovach et al., 1991). There are fewer stabilizing interactions of the aged adducts in the serine proteases than in AChE due to the smaller oxyanion hole and a slight steric clash between the methyl group and Hip57, which cancel some of the favorable electrostatic interactions with Hip57.

We have shown that the dealkylation of the unsolvated P_R diastereomer of isopropyl methylphosphonyl adducts of trypsin would be thermodynamically favored by ~12 kcal/mol (Kovach et al., 1991). The product of dealkylation of this adduct, of course, would be the anionic methylphosphonate ester with the O^- close to Hip57 (Figure 9). This diastereomer is stabilized predominantly by the electrostatic interaction between Hip57 and the O^- but is less accessible to solvate water than the structure in Figure 8. The O^- in this orientation occupies the leaving group binding site in serine proteases (Figure 11). Dealkylation occurred during crystallization of the diisopropyl phosphate adduct of trypsin and produced a monoisopropyl anion adduct in which O^- is in the same place as in Figure 9 [see the X-ray structure by Chambers and Stroud (1977); Kovach, 1988b]. Yet, the configuration at P in the phosphonate ester adducts is predestined to remain intact in the dealkylation process; consequently, the more potent P_S-soman diastereomers, if in-line displacement at P is the favored stereochemistry, would result in the structure shown in Figure 8 and not the more stable one depicted in Figure 9.

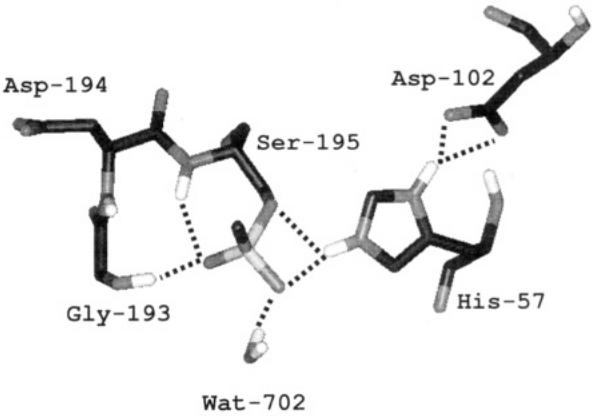

FIGURE 9: Stereochemical relationships at the active site of P_R soman-inhibited trypsin after dealkylation. Dashed lines indicate potential H-bonding interactions at the active site.

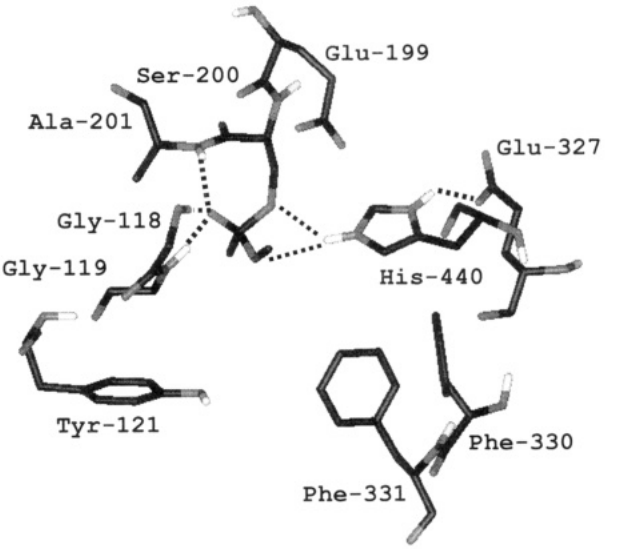

FIGURE 10: Stereochemical relationships within a tetrahedral adduct of AChE with methyl acetate at the active site. Dashed lines indicate potential H-bonding interactions at the active site.

Because of the stronger interaction between Hip57 and the oxyanion in the adduct with P_R configuration, the pK of His57 is expected to rise more for both the diester and monoester (aged) adducts with P_R configuration (Figure 9) than in those with P_S configuration (Figure 8).

Comparison of the Anionic Phosphonate Monoesters of Ser and the Tetravalent Carbonyl Adducts Formed in the Acylation or Deacylation of Each Enzyme. Although the tetrahedral carbonyl fragments are minimal structures and thus lack some of the binding power of the natural substrates, they can mimic the geometries at the reaction center and the electrostatic interactions. The tetrahedral intermediate formed between Ser200 and methyl acetate was oriented to mimic the binding of acetylcholine and P_S-soman, *i.e.*, the location of the methoxy group coincides with that of the choline and the pinacolyl groups (Figure 10). The latter two could not be accommodated in any other conformation without disrupting the oxyanion hole interactions. The oxygen in methoxy is 5.0 Å away from the carboxyl oxygens

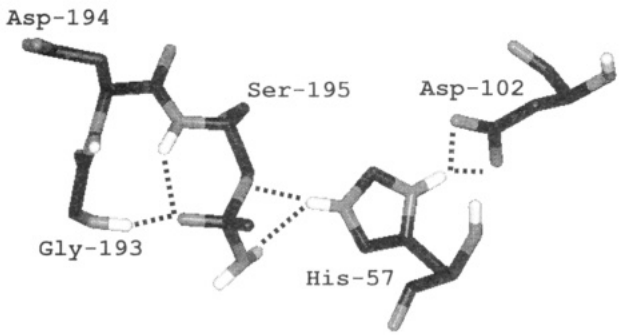

FIGURE 11: Stereochemical relationships within a tetrahedral adduct of trypsin with acetamide at the active site. The orientation of ligands around C corresponds to that in the hydrolysis of a natural substrate and to that in Figure 9.

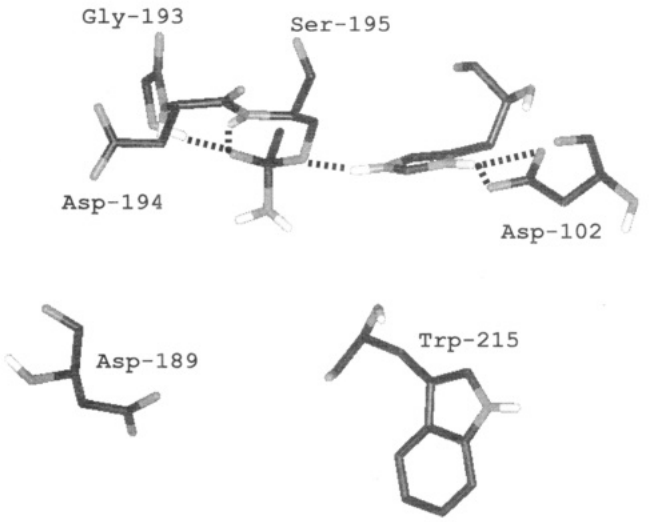

FIGURE 12: Stereochemical relationships within a tetrahedral adduct of trypsin with acetamide at the active site. The orientation of ligands around C corresponds to that in Figure 8.

of Glu199. One may then wonder if Glu199 in AChE has not adapted to also exert an electrostatic "push" at choline and other leaving groups to alleviate the removal of poor leaving groups and thus further boost the catalytic prowess of the enzyme (Kovach, 1988a,b).

Both possible orientations (Figures 11 and 12) were generated for the tetrahedral adduct formed between acetamide and trypsin or chymotrypsin. Although the orientation in Figure 11 mimics the biologically relevant binding, the aged adducts generated via inhibition by the more effective P_S-soman would have the orientation shown in Figure 12. The interaction energies in structures in Figures 11 and 12 were almost the same, except that heteroatoms in the binding pocket were generally more accessible to solvation than at the leaving group binding site. This could be quite different when the specificity pocket is occupied by the appropriate substituent.

The sum of interaction energies between the phosphonyl diester fragments and protein is about the same as that between the carbonyl transients and protein. The interaction energies between the protein and small molecule become markedly more favorable for the anionic monophosphonate adducts than those for the tetravalent carbonyl fragments, by −15.6 kcal/mol for AChE, −20.8 kcal/mol for trypsin, and −12 kcal/mol for chymotrypsin (Table 4). These differences mostly originate from electrostatic interactions between the anionic adducts and polar residues predominantly solvating water molecules. The picture could change with the natural substrates especially when long peptide chains and specificity side chains can bind strongly at their respective binding sites.

CONCLUSIONS

AChE has a more elaborate apparatus in the oxyanion hole and a potentially more versatile acid/base catalytic machinery than the serine proteases, while the latter have a more compartmentalized active site. Differences in the *modus operandi* between the serine protease and AChE group of enzymes serve fulfillment of their different functions: Serine proteases had to evolve to accommodate a long peptide chain, a specific side chain, and a typically long leaving group. In contrast, AChE evolved to catalyze the hydrolysis of a small positively charged substrate, acetylcholine. It performs the task presumably by mobilizing a sophisticated system of negatively charged and hydrophobic residues to bring about both remarkably efficient chemistry and clearance of reactants and products (Kovach et al., 1994). Glu199 has a critical role in the electrostatic catalytic mechanism by "pulling" and possibly "pushing" out the leaving group. It may also serve as a surrogate general base for proton removal from Ser200 in the reaction of bulky substrates. The high local negative charge density, mostly provided by Glu199, and the numerous small van der Waals interactions promote dealkylation of an alkyl methylphosphonate ester of Ser200 much more effectively than any other similar enzyme. Moreover, the high concentration of negative charge created by the phosphonate ester monoanion and Glu199 adjacent to it surrounding the only accessible side of the central P fully accounts for the resistance to the attack of even the strongest nucleophile applied for enzyme reactivation. The phosphoryl and anionic oxygens each carry ~0.75 unit fractional negative charge, which is significantly greater than at the oxygens of tetravalent carbonyl adducts. This results in 12−22 kcal/mol worth of stabilizing interactions in the phosphonate monoester anions of Ser relative to the tetrahedral intermediate of small carbonyl compounds. The phosphonate monoester anions are stabilized by three H-bonds, and the corresponding electrostatic forces in the oxyanion hole, and by Hip440. Stereoselectivity of AChE for soman is mostly governed by steric effects, while the dealkylation reaction is almost equally likely for all diastereomers of the phosphonyl-AChE. The differences in stability of the diasteromeric adducts are less in the soman-inhibited serine proteases, but the tendency for dealkylation seems greater for the P_R diastereomers.

ACKNOWLEDGMENT

We thank Dr. B. R. Brooks at NIH/DCRT for many helpful suggestions and for access to the HP 735 cluster.

REFERENCES

Adebodun, F., & Jordan, F. (1989) *J. Cell. Biochem. 40*, 249.

Aldridge, W. N., & Reiner, E. (1972) *Enzyme Inhibitors as Substrates: Interactions of Esterases with Organophosphorus and Carbamic Acids*, American Elsevier, New York.

Allen, F. H., Bellard, S., Brice, M. D., Cartwright, B. A., Doubleday, A., Higgs, H., Hummelink, T., Hummelink-Peters, B. G., Kennard, O., Motherwell, W. D. S., Rodgers, J. R., & Watson,

D. G. (1979) *Acta Crystallogr., Sect. B B35*, 2331.
Bachovchin, W. W. (1986) *Biochemistry 25*, 7751.
Barnard, E. (1974) in *The Peripheral Nervous System* (Hubbard, J. I., Ed.) pp 201−224, Plenum, New York.
Bencsura, A., Enyedy, I., Viragh, C., Akhmetshin, R., & Kovach, I. M. (1995) in *Proceedings of the Fifth International Meeting on Cholinesterases, Madras, India* (Quinn, M. D., & Doctor, B. P., Eds.) Plenum Publishing Co., Amsterdam.
Bender, M. L., & Wedler, F. C. (1972) *J. Am. Chem. Soc. 94*, 2101.
Bennet, A. J., Kovach, I. M., & Schowen, R. L. (1988) *J. Am. Chem. Soc. 110*, 7892.
Bennet, A. J., Kovach, I. M., & Bibbs, J. A. (1989) *J. Am. Chem. Soc. 111*, 6424.
Berman, H. A. (1995) in *Proceedings of the Fifth International Meeting on Cholinesterases, Madras, India* (Quinn, M. D., & Doctor, B. P., Eds.) Plenum Publishing Co., Amsterdam.
Berman, H. A., & Decker, M. M. (1986) *J. Biol. Chem. 261*, 10646.
Bernstein, F., Koetzle, T. F., Williams, G. J. B., Meyer, E. F., Jr., Brice, M. D., Rodgers, J. R., Kennard, O., Shimanouchi, T., & Tasumi, M. J. (1977) *J. Mol. Biol. 112*, 535.
Bizozero, S. A., & Dutler, H. (1981) *Bioorg. Chem. 10*, 46.
Blow, D. M., Birktoft, J. J., & Hartley, B. S. (1969) *Nature 221*, 337.
Brooks, B. R., Bruccoleri, R. E., Olafson, B. D., States, D. J., Swaminathan S., & Karplus, M. (1983) *J. Comput. Chem. 4*, 187.
Broomfield, C. A., Wingertsahn, S., Grothusen, J. R., Clark, J. H., Green, M. D., Brown, T. M., & Lieske, C. N. (1984) *Book of Abstracts*, 188th National Meeting of the American Chemical Society, Philadelphia, PA, Abstract BIOL 28.
Buchwald, S. L., Hansen, D. E., Hassett, A., & Knowles, J. R. (1982) *Methods in Enzymol. 89*, 279.
Cammissa, J., Kim, J. R., & Lee, B. K. (1992) *GEMM Program Version 7.87, Molecular Modeling Section*, NIH, Bethesda, MD 20892.
Chambers, J. L., & Stroud, R. M. (1977) *Acta Crystallogr., Sect. B B33*, 1824.
Cohen, W., Lache, M., & Erlanger, B. F. (1962) *Biochemistry 1*, 686.
Cygler, M., Schrag, J. D., Sussman, J. L., Harel, M., Silman, I., Gentry, M. K., & Doctor, B. P. (1993) *Protein Sci. 2*, 366.
de Jong, L. P. A., & Benschop, H. P. (1988) in *Stereoselectivity of Pesticides* (Ariens, E. J., van Rensen, J. J. S., & Welling, W., Eds.) pp 109−149, Elsevier, Amsterdam.
Dewar, S., Zoebisch, E. G., Healy, E. F., & Stewart, J. J. P. (1985) *J. Am. Chem. Soc. 107*, 3902.
Frank, R., & Usher, A. S. (1967) *J. Am. Chem. Soc. 89*, 6360.
Frey, P. A., Whitt, S. A., & Tobin, J. B. (1994) *Science 264*, 1927.
Gilson, M. K., Straatsma, J. A., McCammon, J. A., Ripoll, D. R., Faerman, C. H., Axelsen, P. H., Silman, I., & Sussman, J. L. (1994) *Science 263*, 1276.
Gorenstein, D. G., Shah, D., Chen, R., & Kallick, D. (1989) *Biochemistry 28*, 2050.
Green, A. L., & Nicholls, J. D. (1959) *Biochem. J. 72*, 70.
Grunwald, J., Segall, Y., Shirin, E., Waysbort, D., Steinberg, N., Silman, I., & Ashani, Y. (1989) *Biochem. Pharmacol. 38*, 3157.
Hartley, B. S., & Kilby, B. A.(1952) *Biochem. J. 50*, 672.
Hartley, B. S., & Kilby, B. A. (1954) *Biochem. J. 56*, 288.
Johnson, M. K. (1980) *Nature 287*, 105.
Jorgensen, W. L., Chandrasekhar, J., Madura, J. D., Impey, R. W., & Klein, M. L. (1983) *J. Chem. Phys. 79*, 926.
Keijer, J. H., & Wolring, G. Z. (1969) *Biochim. Biophys. Acta 185*, 465.
Kossiakoff, A. A., & Spencer, S. A. (1981) *Biochemistry 20*, 6462.
Kovach, I. M. (1988a) *J. Enzyme Inhib. 2*, 199.
Kovach, I. M. (1988b) *Theochem 76*, 159.
Kovach, I. M., & Schowen, R. L. (1987) in *Peptides and Proteases: Recent Advances* (Schowen, R. L., & Barth, A., Eds.) p 205, Pergamon, Oxford.
Kovach, I. M., & Huhta, D. (1991) *Theochem. 79*, 335.
Kovach, I. M., Larson, M., & Schowen, R. L. (1986a) *J. Am. Chem. Soc. 108*, 3054.
Kovach, I. M., Larson, M., & Schowen, R. L. (1986b) *J. Am. Chem. Soc. 108*, 5490.
Kovach, I. M., Huber-Ashley, H. J., & Schowen, R. L. (1988) *J. Am. Chem. Soc. 110*, 590.
Kovach, I. M., Huhta, D., & Baptist, S. J. (1991) *Theochem 72*, 99.
Kovach, I. M., McKay, L., & Vander Velde, D. (1993) *Chirality*, 143.
Kovach, I. M., Qian, N., & Bencsura, A. (1994) *FEBS Lett. 349*, 60.
Lienhard, G. E. (1973) *Science 180*, 149.
Main, A. R. (1979) *Pharmacol. Ther. 6*, 579.
Michael, H. O., Hackley, B. E., Jr., Berkovitz, L., List, G., Hackley, E. B., Gillilan, W., & Pankau, M. (1967) *Arch. Biochem. Biophys. 121*, 29.
Nair, K. H., Seravalli, J., Arbuckle, T., & Quinn, D. M. (1994) *Biochemistry 33*, 8566.
Nakagawa, S., Yu, H., Karplus, M., & Umeyama, H. (1993) *Proteins: Struct., Funct., Genet. 16*, 172.
Ordentlich, A., Kronman, C., Barak, D., Stein, D., Ariel, N., Marcus, D., Velan, B., & Shafferman, A. (1993) *FEBS Lett. 334*, 215−220.
Polgar, L. (1987) in *Hydrolytic Enzymes* (Neuberger, A., & Brocklehurst, K., Eds.) Elsevier, Amsterdam.
Qian, N., & Kovach, I. M. (1993) *FEBS Lett. 336*, 263.
Quinn, D. M. (1987) *Chem. Rev. 87*, 955.
Quinn, D. M., Pryor, A. N., Selwood, T., Lee, B. H., Acheson, S. A., & Barlow, P. N. (1991) in *Cholinesterases: Structure, Function, Mechanism, Genetics, and Cell Biology* (Massoulie, J., Bacou, F., Barnard, E., Chatonnet, A., Doctor, B. P., Quinn, D. M., Eds.) American Chemical Society, Washington, DC.
Ripoll, D. R., Faerman, C. H., Axelsen, P. H., Silman, I., & Sussman, J. L. (1993) *Proc. Natl. Acad. Sci. U.S.A. 90*, 5128.
Rozenberry, T. L. (1975) *Adv. Enzymol. 43*, 103.
Saxena, A., Doctor, B. P., Maxwell, D. M, Lenz, D. E., Radic, Z., & Taylor, P. (1993) *Biochem. Biophys. Res. Commun. 197*, 343.
Schoene, K., Steinhanses, J., & Wertman, A. (1980) *Biochim. Biophys. Acta 616*, 384.
Segall, Y., Waysbort, D., Barak, D., Ariel, N., Doctor, B. P., Grunwald, J., & Ashani, Y. (1993) *Biochemistry 32*, 3441.
Selwood, T., Feaster, S. R., States, M. J., Pryor, A. N., & Quinn, D. M. (1993) *J. Am. Chem. Soc. 115*, 10477.
Singh, U. C., Weiner, P. K., Caldwell, J. W., & Kollman, P. A. (1986) *AMBER (UCSF Version 3.0)*, Department of Pharmaceutical Chemistry, University of California, San Francisco.
Smith, T. E., & Usdin, E. (1966) *Biochemistry 5*, 2914.
Sussman, J. L., Harel, M., Frolow, F., Oefner, C., Goldman, A., Tokder, L., & Silman, I. (1991) *Science 253*, 872.
Tan, R. C., Troung, T. N., McCammon, J. A., & Sussman, J. L. (1993) *Biochemistry 32*, 401.
Van der Drift, A. C. M., Beck, H. C., Dekker, W. H., Hulst, A. G., & Wils, E. R. (1985) *Biochemistry 24*, 6894.
Vedani, A. (1990) *J. Am. Chem. Soc. 112*, 4759.
Venkatasubban, K. S., & Schowen, R. L. (1987) *CRC Crit. Rev. Biochem. 17*, 1.
Westheimer, F. H. (1968) *Acc. Chem. Res. 1*, 70.
Zhao, Q., Kovach, I. M., Bencsura, A., & Papathanassiu (1994) *Biochemistry 33*, 8124.

BI950162L